

# Photoproduction of the $\eta$ Meson from the Deuteron Near Threshold \*

CH. ELSTER<sup>1,2</sup>, A. SIBIRTSEV<sup>1</sup>, S. SCHNEIDER<sup>1</sup>, J. HAIDENBAUER<sup>1</sup>,  
S. KREWALD<sup>1</sup> AND J. SPETH<sup>1</sup>

<sup>1</sup>Institut für Kernphysik, Forschungszentrum Jülich, D-52425 Jülich

<sup>2</sup>Department of Physics and Astronomy, Ohio University, Athens, OH 45701

Very recent data for the reaction  $\gamma d \rightarrow \eta np$  are analyzed within a model that includes contributions from the impulse approximation and next order corrections due to the  $np$  and  $\eta N$  interactions in the final state. Comparison between the calculations and data indicate sizable contributions from the  $np$  and  $\eta N$  final state interactions close to threshold.

PACS numbers: 13.60Le, 13.75.Cs, 14.40.Aq, 14.20.Gk

## 1. Introduction

Reactions at threshold are often investigated to learn about the interactions between the reaction products. The study of meson production close to threshold has several peculiar features. Only a very limited part of the phase space is available for the reaction products, hence, only a few partial waves contribute to the observables. However, the small phase space also yields small cross sections. In the entrance channel one deals with large momenta, but only with small momenta in the final meson-baryon system.

Indeed, a strong influence of the final state interaction (FSI) on the cross sections of  $\pi$ ,  $\eta$ ,  $\eta'$  and  $\omega$ -meson production in nucleon-nucleon ( $NN$ ) collisions was observed in experiments at the IUCF, COSY and CELSIUS accelerator facilities [1, 2, 3, 4, 5]. With the exception of the  $\eta$  channel, those experiments producing mesons in  $NN$  collisions can be described almost perfectly by theoretical calculations accounting only for the final state interactions between the nucleons [4, 5]. In case of  $\eta$  production there is evidence that the  $\eta N$  FSI could play a role as well [2].

---

\* Presented at the 7th International Workshop on Meson Production, Properties and Interaction, May 24-28 2002, Krakow, Poland

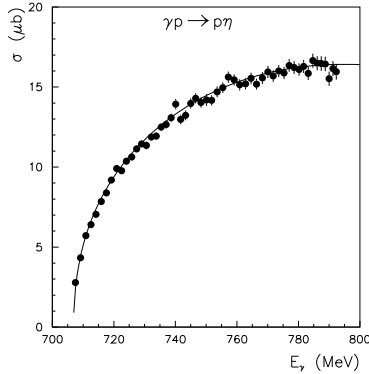


**Fig.1:** Total cross section for the reaction  $\gamma p \rightarrow p\eta$ . The experimental data are from [7], while the solid line gives our result.

Here the reaction  $\gamma d \rightarrow np\eta$  [6] close to the meson production threshold is studied. It offers an opportunity to investigate the final state interactions between the outgoing particles: proton, neutron, and  $\eta$  meson. Provided the FSI between the nucleons is understood, the reaction allows us to draw conclusions about the  $\eta N$  interaction at low energies. In Refs. [8, 9, 10] we investigated incoherent  $\eta$  photoproduction from the deuteron close to threshold taking into account that the reaction amplitude is given by the sum of the first order term, the impulse approximation (IA), and the terms of the next higher order due to the final state interactions in the neutron-proton ( $np$ ) and the  $\eta$ -nucleon ( $\eta N$ ) system.

As  $np$  interaction we employ one of the high-precision  $NN$  potentials, the CD-Bonn potential [11]. The  $\eta N$  interaction is extracted from an effective, microscopic coupled channel model for  $\pi N$  scattering developed by the Jülich group [12, 13]. This model includes the  $\eta N$  channel and quantitatively describes the  $\pi N$  phase shifts and inelasticity parameters in both isospin channels for partial waves up to  $J = \frac{3}{2}$  and pion-nucleon center-of-mass (c.m.) energies up to 1.9 GeV [13]. Specifically, it provides a realistic description of the quantities relevant for the present investigation, namely the  $S_{11}$   $\pi N$  phase shift and the  $\pi N \rightarrow \eta N$  transition cross section. Calculations in the same spirit were carried out earlier [14], however there the  $\eta N$  interaction was treated in a separable ansatz. In Sec. 2 we discuss our calculations of the reaction  $\gamma d \rightarrow \eta N$ . In Sec. 3 we give a phenomenologically based discussion of the enhancement of  $\eta$  meson production in pp collisions in comparison with our results, and we conclude in Sec. 4.

## 2. The Reaction $\gamma d \rightarrow np\eta$

### 2.1. The Elementary Amplitude and the Impuls Approximation

The dominant contribution to the  $\eta$ -meson photoproduction from a single nucleon is given by the  $N^*$  isobar excitation [15, 16]. Since there is no strong experimental evidence [17] for contributions to  $\eta$ -meson photoproduction from resonances other than the  $S_{11}(1535)$  isobar in the near-threshold region, we consider only this resonance. The partial decay widths,

$S_{11}(1535) \rightarrow N\eta$  and  $S_{11}(1535) \rightarrow N\pi$ , are related to the relevant coupling constant  $g_{RN\xi}$ ,  $\xi=\eta, \pi$ , by

$$\Gamma_\xi = \frac{g_{RN\xi}^2}{4\pi} \frac{q_\xi(E_N + m_N)}{M_R}. \quad (1)$$

Here the momentum  $q_\xi$  and the nucleon energy  $E_N$  are evaluated in the rest frame of the resonance at the pole position of  $S_{11}(1535)$ . Considering only the contribution of the  $S_{11}(1535)$  resonance, the data for  $\eta$ -meson photoproduction off protons can be well fitted with the following resonance parameters at the  $S_{11}(1535)$  pole:  $M_R = 1544 \text{ MeV}$ ,  $\Gamma = 203 \text{ MeV}$ ,  $\Gamma_\eta/\Gamma = 0.45$ ,  $\Gamma_\pi/\Gamma = 0.45$ ,  $\Gamma_{\pi\pi}/\Gamma = 0.1$ . Further details are given in Ref. [8]. The calculation of the cross section for the reaction  $\gamma p \rightarrow p\eta$  is shown in Fig. 1 in comparison with the data.

Using the impulse approximation (IA) the amplitude  $\mathcal{M}_{IA}$  of the reaction  $\gamma d \rightarrow np\eta$  for given spin  $S$  and isospin  $T$  of the final nucleons can be written as

$$\mathcal{M}_{IA} = A^T(s_1)\phi(p_2) - (-1)^{S+T} A^T(s_2)\phi(p_1). \quad (2)$$

Here  $\phi(p_i)$  stands for the deuteron wave function,  $p_i$  ( $i = 1, 2$ ) is the momentum of the proton or neutron in the deuteron rest frame, and  $A^T$  denotes the isoscalar or isovector  $\eta$ -meson photoproduction amplitude at the squared invariant collision energy  $s_N$  given by

$$s_N = s - m_N^2 - 2(E_\gamma + m_d)E_N + 2\vec{k}_\gamma \cdot \vec{p}_i. \quad (3)$$

The photon momentum is given by  $\vec{k}_\gamma$ , and  $s = m_d^2 + 2m_dE_\gamma$  stands for the square of the invariant mass. Details of the photoproduction amplitude  $A^T$  are described in Ref.[8]. The result for the total cross section for the reaction  $\gamma d \rightarrow np\eta$  based on the impulse approximation is shown as dotted line in Fig. 2 in comparison to experiment. Though the impulse approximation describes the data above  $\approx 680$  MeV rather well, close to threshold it underestimates them substantially.

## 2.2. The Final State Interactions

The amplitude  $\mathcal{M}_{NN}$  for the  $np$  final state interaction is given by

$$\mathcal{M}_{NN} = m_N \int dk k^2 \frac{t_{NN}(q, k) A^T(s'_N) \phi(p'_N)}{q^2 - k^2 + i\epsilon}, \quad (4)$$

where  $q$  is the nucleon momentum in the final  $np$  system and

$$\vec{p}'_N = \vec{k} + \frac{\vec{k}_\gamma - \vec{p}_\eta}{2}, \quad (5)$$

$p_\eta$  is the  $\eta$ -meson momentum and  $p'_N = |\vec{p}'_N|$ . The half-shell  $np$  scattering matrix  $t_{NN}(q, k)$  in the  $^1S_0$  and  $^3S_1$  partial waves was obtained at corresponding off-shell momenta  $k$  from the CD-Bonn potential [11]. Finally, the amplitude  $\mathcal{M}_{\eta N}$  for the  $\eta N$  final state interaction is given as

$$\mathcal{M}_{\eta N} = \frac{m_N m_\eta}{m_N + m_\eta} \int dk k^2 \frac{t_{\eta N}(q, k) A^T(s''_N) \phi(p''_N)}{q^2 - k^2 + i\epsilon}, \quad (6)$$

where the  $\eta$ -meson momenta in the final and intermediate state of the  $\eta N$  system are indicated by  $q$  and  $k$ ,  $t_{\eta N}(q, k)$  is the half-shell  $\eta N$  scattering matrix in the  $S_{11}$  partial wave and

$$\vec{p}''_N = \vec{k} + \frac{m_N (\vec{k}_\gamma - \vec{p}'_N)}{m_N + m_\eta}, \quad (7)$$

where  $\vec{p}'_N$  is the momentum of the final proton or neutron in the deuteron rest frame and  $m_\eta$  is the  $\eta$ -meson mass.

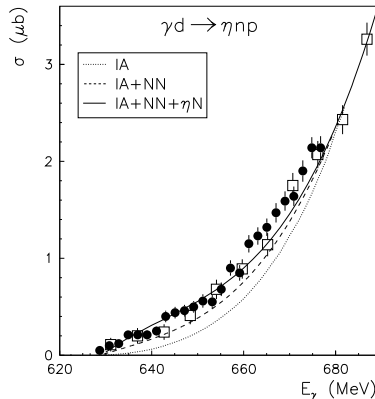


**Fig.2:** The total cross section for inclusive photoproduction of  $\eta$  mesons off deuterium as function of the photon energy  $E_\gamma$ . The data are from [6] (full circles) and [7] (open squares). The dotted line represents the IA calculation, while the dashed line is the result with the  $np$  final state interaction. The solid line shows the full calculation, including the  $\eta N$  final state interaction from the Jülich meson-baryon model [9].

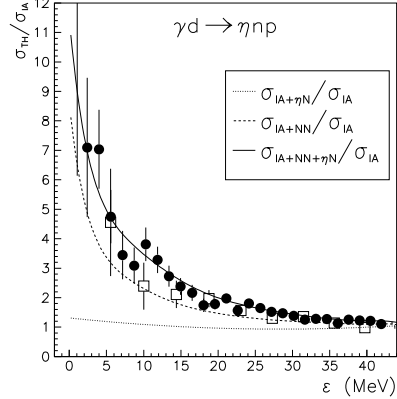


**Fig.3:** The cross section ratios for inclusive photon production of  $\eta$ -mesons off the deuteron as a function of the excess energy  $\varepsilon = \sqrt{s} - m_p - m_n - m_\eta$ . Shown are our calculations including the indicated final state interactions divided by the impulse approximation. The solid line indicates the full calculation containing  $np$  and  $\eta N$  FSI. The dashed line stands for a calculation including only the  $np$  FSI, whereas the calculation for the dotted line includes only the  $\eta N$  FSI.

The total cross section  $\gamma d \rightarrow np\eta$  including the  $np$  and  $\eta N$  FSI in S waves

is displayed in Fig. 2. The dashed line shows the result for the IA plus  $np$  FSI, and the solid line includes in addition the  $\eta N$  FSI, as given by the Jülich meson-baryon model. As expected, the attractive  $\eta N$  FSI enhances the cross section very close to the reaction cross section. We observe that for photon energies larger than 670 MeV there is hardly any effect of the  $\eta N$  FSI any longer. The same is true for the  $np$  FSI. Fig. 2 shows that we can well describe the data close to the reaction threshold, while there is a systematic underprediction of about 10% of the experimental results between 660 and 680 MeV photon energy. However, we should not attribute this discrepancy to the  $\eta N$  FSI, since we found in Ref. [9] that the  $\eta N$  interaction acts predominantly very close to threshold. We also want to point out that our calculation matches up with the older data (open squares) at energies larger than 680 MeV.

It is illuminating to look at the difference in the relative strength of the two different final state interactions and their possible interference in our full calculation of the  $\eta$  photoproduction cross section. For a more detailed insight, we plot in Fig. 3 the ratio of calculations with the final state interactions included separately to the calculation based on the impulse approximation alone. The dotted line in Fig. 3 represents the calculation including only the  $\eta N$  FSI, the dashed line only the  $np$  FSI. From this, it is clear that the  $np$  FSI is the dominant one, a finding already reported in Ref. [14]. The ratio of the full calculation containing both, the  $\eta N$  and  $np$  FSI, to the impulse approximation is given by the solid line. A comparison to the two other curves shows that the two final state interactions interfere constructively at small excess energies, which magnifies the effect of the relatively weak  $\eta N$  FSI.

When characterizing low energy properties of the  $\eta N$  interaction within the effective range approximation, the  $\eta N$  on-shell scattering matrix is related to the scattering length  $a_{\eta N}$  as

$$\left[ iq - \frac{1}{a_{\eta N}} \right]^{-1} = \pi \frac{\sqrt{q^2 + m_N^2} \sqrt{q^2 + m_\eta^2}}{\sqrt{q^2 + m_N^2 + \sqrt{q^2 + m_\eta^2}}} t_{\eta N}(q, q). \quad (8)$$

In previous work [9] we showed that within our approach the uncertainty of the calculations is dominated by the insufficient knowledge of the strength of the  $\eta N$  interaction, here represented by  $a_{\eta N}$ . Moreover, possible effects due to higher order corrections from the multiple scattering expansion [18, 19] might be overshadowed by the sizable variation of  $a_{\eta N}$ , which as a result of different model calculations or extractions can range from  $0.25+i0.16$  to  $1.05+i0.27$  fm. The Jülich meson-baryon model, whose t-matrix,  $t_{\eta N}(q, k)$ , we adopt in our calculations leads to a scattering length  $a_{\eta N}=0.42+i0.32$  fm, which is roughly in the mid-range of the values suggested in the literature.

In Ref. [9] we showed that within our model this value of the scattering length results from the interplay of resonant,  $N^*(1535)$ , and nonresonant contributions.

We also explored how strongly our calculation of the  $\eta N$  FSI depends on the specific properties of the  $\eta N$  interaction. In order to study whether there is sensitivity to the off-shell behavior we carried out calculations where the  $\eta N$  amplitude of Eq. (6) is replaced by its effective range expansion of Eq. (8). Surprisingly, we obtained identical results for the  $\eta$  photoproduction cross section when using either the  $\eta N$  t-matrix from the effective range expansion or the one from the full model. This can be explained through the relatively good representation of the  $\eta N$  scattering amplitude by the effective range expansion up to momenta  $q \approx 350$  MeV, as well as the very weak  $k$  dependence of the half-shell  $\eta N$  t-matrix,  $t_{\eta N}(q, k)$  [9].

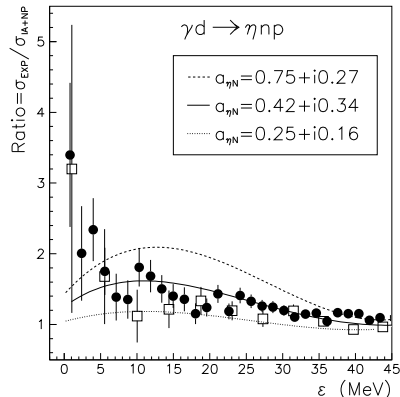


**Fig.4:** The cross section for the reaction  $\gamma d \rightarrow np\eta$  as function of the excess energy  $\varepsilon$ . Shown is the experimental cross section divided by our calculation containing IA and  $np$  FSI. The solid line indicates our full calculation divided by the calculation based on IA and  $np$  FSI only. The dotted and dashed lines show calculations employing the scattering lengths indicated in the figure for the  $\eta N$  FSI. The notation for the data is the same as in Fig. 2.

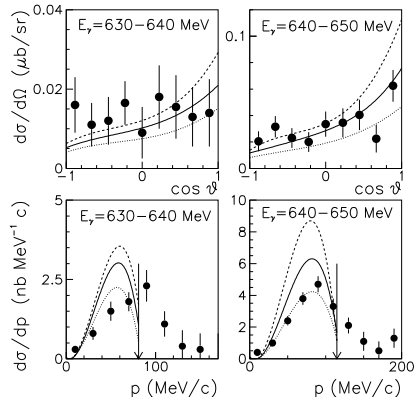


**Fig.5:** The angular (upper part) and momentum (lower part) spectra of  $\eta$ -mesons in the photon-deuteron c.m. system at photon energies  $E_\gamma = 630-640$  and  $640-650$  MeV. The data are from Ref. [6]. The lines show our calculations with different  $\eta N$  scattering lengths, namely  $a_{\eta N} = 0.42 + i0.32$  (solid),  $0.74 + i0.27$  (dashed) and  $0.25 + i0.16$  fm (dotted). The arrows indicate the kinematical limit for  $\eta$ -meson momenta.

The next logical step is to see whether some more quantitative information about the strength of the  $\eta N$  interaction at low energies can be obtained from the photoproduction reaction. Since we found that the  $\eta N$  amplitude

obtained with the effective range expansion is numerically identical to the full calculation of the amplitude, we can explore the effect of different values for the  $\eta N$  low energy parameters on the cross section and momentum distributions close to threshold. In Figs. 4 and 5 we display the calculation with our model together with two calculations with scattering lengths  $a_{\eta N}=0.25+i0.16$  fm [20] (dotted line) and  $a_{\eta N}=0.74+i0.27$  fm [21] (dashed line). The figures suggest that the presently available data for  $\varepsilon \leq 40$  MeV show a preference for smaller values of the  $\eta N$  scattering length. Similar indications for a preference for a smaller value of the  $a_{\eta N}$  have recently been found in calculations for the reaction  $np \rightarrow d\eta$  close to threshold [22].

### 3. Phenomenological Consideration of the $\eta N$ FSI in the Reaction $pp \rightarrow pp\eta$

In the previous section we showed that the  $\eta N$  final state interaction gives a non negligible contribution to the cross section of the reaction  $\gamma d \rightarrow np\eta$ . Calculations of the reaction  $np \rightarrow d\eta$  near threshold also exhibits considerable sensitivity to the  $\eta N$  interaction. One can now ask, if there is some experimental indication, that the  $\eta N$  FSI is also visible close to threshold in the reaction  $pp \rightarrow pp\eta$ . Recent calculations [23] of that reaction include the contribution of the  $pp$  FSI but not yet the one of the  $\eta N$  FSI. Due to the lack of ab initio calculations, one can try if the data themselves reveal indications of a contribution of the  $\eta N$  FSI.

For our estimate of the contribution of the  $\eta N$  FSI in the reaction  $\gamma d \rightarrow np\eta$ , we divide our full calculation by the calculation that contains only the IA and the  $np$  FSI, see Fig. 4. The deviation from 1 can then be interpreted as the contribution of the  $\eta N$  FSI. In order to proceed in a similar fashion in the reaction  $pp \rightarrow pp\eta$  we first need to extract the contribution of the  $pp$  FSI. Since we want to give here phenomenological arguments and do not want to depend on a specific model, we try to extract it from experiment. For this, we consider the total cross section of the reaction  $pp \rightarrow pp\pi^0$ , and parameterize the  $pp$  FSI assuming that the deviation from the phase space is a quadratic function of the excess energy  $\varepsilon$ . For small excess energies ( $\leq 40$  MeV) this is certainly justified. The experimental data for the reaction  $pp \rightarrow pp\pi^0$  are shown in Fig. 6a. The solid line represents the fit to the deviation from phase space and is given by

$$f(\varepsilon) = \left( \frac{6}{1 + 0.042\varepsilon^2} + 1 \right) \cdot \varepsilon^2 \cdot 0.0016, \quad (9)$$

where the last value is given in  $\mu b$ . The reaction  $pp \rightarrow pp\pi^0$  is chosen, since it is known that the  $\pi N$  FSI is negligible.

Having determined the function  $f(\varepsilon)$  representing the  $pp$  FSI, we divide the data for the reaction  $pp \rightarrow pp\eta$  by  $f(\varepsilon)$  and normalize the quotient to 1 at an excess energy  $\varepsilon \approx 100$  MeV, i.e. far enough away from the reaction threshold.

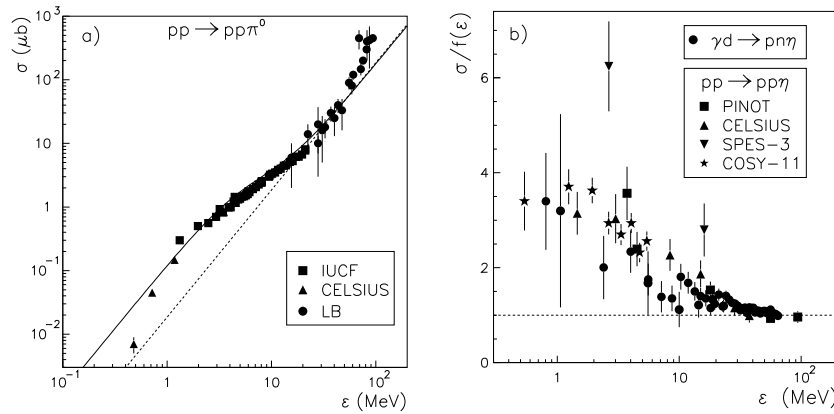


**Fig.6:** The left panel (a) shows the cross section for the reaction  $pp \rightarrow pp\pi^0$ . The solid line gives the function  $f(\varepsilon)$  taking into account a deviation from the phase space proportional to  $\varepsilon^2$ . The data are from: squares [1], triangles [24], circles [25]. The right panel (b) shows the total cross section for the reaction  $pp \rightarrow pp\eta$  close to threshold, where the data are divided by the function  $f(\varepsilon)$ . Our calculation for the cross section of the reaction  $\gamma d \rightarrow np\eta$ , divided by our calculation based on the IA and the  $np$  FSI alone, are shown by the filled circles. The experimental data are: squares [26], upward triangles [2], downward triangles [27], and stars [28].

The resulting cross section ratios are depicted in Fig. 6b. For excess energies  $\varepsilon \leq 10$  MeV the data for the reaction  $pp \rightarrow pp\eta$  indicate an enhancement of the cross section. This enhancement is very similar to the one we find in the reaction  $\gamma d \rightarrow np\eta$ . For comparison, we plotted those data also in Fig. 6b, and surprisingly, the enhancement seen in the photoproduction is of the same order of magnitude as the one phenomenologically extracted from the hadronic reaction. Of course, the effect of the  $\eta N$  FSI has to be calculated theoretically for the reaction  $pp \rightarrow pp\eta$  in order to draw definite conclusions.

#### 4. Summary

We calculated the reaction  $\gamma d \rightarrow np\eta$ , including the dominant contribution by the  $S_{11}$  resonance in the elementary amplitude and the final state

interactions between all outgoing particles. Those final state interactions influence the cross section for inclusive photoproduction only for excess energies of the  $\eta$  meson smaller than 40 MeV. At higher energies the cross section is given solely by the impulse approximation.

The FSI between the outgoing nucleons is essential to bring the calculated cross section into the vicinity of the experimental values. Our calculations are based on the CD-Bonn potential, however due to the presence of the deuteron wave function in the expression of the FSI amplitude, possible off-shell differences of various  $NN$  potential do not enter the amplitude. Due to a constructive interference effect the  $\eta N$  final state interaction provides an additional enhancement of the production cross section at energies close to threshold, as required by the data. In our calculations we use the  $\eta N$  interaction extracted from the Jülich meson-baryon model. We found that the effect of the FSI resulting from the  $\eta N$  interaction can be very well incorporated into the model by resorting to an effective range approximation fitted to the full scattering amplitude of the  $\eta N$  model. Guided by this finding, we considered  $\eta N$  final state interactions given by effective range expansions with different values for the scattering length, and concluded that presently available data for the reaction  $\gamma d \rightarrow np\eta$  are consistent with moderate values of the real part of the scattering length  $a_{\eta N}$ . This finding is consistent with a recent calculation of the reaction  $np \rightarrow d\eta$ .

## REFERENCES

- [1] H.O. Meyer et al., Phys. Rev. Lett. **65**, 2846 (1990); H.O. Meyer et al., Nucl. Phys. A **539**, 633 (1992).
- [2] H. Calén et al., Phys. Lett. B **366**, 39 (1996); Phys. Rev. Lett. **80**, 2069 (1998).
- [3] P. Moskal et al., Phys. Rev. Lett. **80**, 3202 (1998); P. Moskal et al., Phys. Lett. B **474**, 416 (2000).
- [4] P. Moskal et al., Phys. Lett. B **482**, 356 (2000).
- [5] For an overview and further references see, e.g., H. Machner and J. Haidenbauer, J. Phys. G **25**, R231 (1999).
- [6] V. Hejny et al., Eur. Phys. J. A **13**, 493, (2002).
- [7] B. Krusche et al., Phys. Lett. B **358**, 40 (1995).
- [8] A. Sibirtsev, Ch. Elster, J. Haidenbauer, J. Speth, Phys. Rev. C **64**, 024006 (2001).
- [9] A. Sibirtsev, S. Schneider, Ch. Elster, J. Haidenbauer, S. Krewald and J. Speth, Phys. Rev. C **65**, 044007 (2002).
- [10] A. Sibirtsev, S. Schneider, Ch. Elster, J. Haidenbauer, S. Krewald and J. Speth, Phys. Rev. C **65**, 067002 (2002).
- [11] R. Machleidt, Phys. Rev. C **63**, 024001 (2001).

- [12] C. Schütz, J. Haidenbauer, J. Speth, and J.W. Durso, Phys. Rev. C **57**, 1464 (1998).
- [13] O. Krehl, C. Hanhart, S. Krewald, J. Speth, Phys. Rev. C **62**, 025207 (2000).
- [14] A. Fix and H. Arenhövel, Z. Phys. A **359**, 427 (1997).
- [15] G. Knöchlein, D. Drechsel and L. Tiator, Z. Phys. A **352**, 327 (1995)
- [16] M. Benmerrouche and N.C. Mukhopadhyay, Phys. Rev. D **51**, 3237 (1995).
- [17] Particle Data Group, Eur. Phys. J. C **15**, 1 (2000).
- [18] R. Delborgo, Nucl. Phys. **38**, 249 (1962).
- [19] J. Gillespie, Final State Interactions, Holden-Day (1964) 91.
- [20] C. Bennhold and H. Tanabe, Nucl. Phys. A **530**, 625 (1991).
- [21] A.M. Green and S. Wycech, Phys. Rev. C **55**, R2167 (1997).
- [22] H. Garcilazo, M.T. Pena, private communication.
- [23] K. Nakayama, J. Speth, T.-S.H. Lee, Phys. Rev. C **65**, 045210 (2002).
- [24] A. Bondar *et al.*, Phys. Lett **B356**, 8 (1995).
- [25] Landolt-Börnstein, New Series I/12, edited by H. Schopper, Springer (1988).
- [26] E. Chiavarra *et al.*, Phys. Lett **B322**, 270 (1994).
- [27] A.M. Bergdolt *et al.*, Phys. Rev. D **48**, 2966 (1993).
- [28] J. Smyrski *et al.*, Phys. Lett **B474**, 182 (2000).